ORIGINAL ARTICLE

Modelling the Role of Tax Expression in HTLV-I Persistence in vivo

Michael Y. Li · Aaron G. Lim

Abstract Human T-lymphotropic virus type I (HTLV-I) is a persistent human retrovirus characterized by life-long infection and risk of developing HAM/TSP, a progressive neurological and inflammatory disease, and adult T-cell leukemia (ATL). Chronically infected individuals often harbor high proviral loads despite maintaining a persistently activated immune response. Based on a new hypothesis for the persistence of HTLV-I infection, a three-dimensional compartmental model is constructed that describes the dynamic interactions among latently infected target cells, target-cell activation, and immune responses to HTLV-I, with an emphasis on understanding the role of Tax expression in the persistence of HTLV-I.

Keywords Mathematical modelling · HTLV-I · Persistent viral infection · Latently infected target cells · Viral tax protein · Global stability · Backward bifurcation

1 Introduction

Human T-lymphotropic virus type I (HTLV-I) is the aetiological agent of HTLV-I-associated myelopathy or tropical spastic paraparesis (HAM/TSP) (Gallo 2005), and infection can also lead to adult T-cell leukemia/lymphoma (ATL) (Proietti et al. 2005). HTLV-I infection is life-long and there is currently no cure nor preventative vaccine for HTLV-I, and neither is there satisfactory treatment for HTLV-I-associated pathologies (Bangham 2000; Proietti et al. 2005). The majority of HTLV-I-infected

M.Y. Li
Department of Mathematical and Statistical Sciences, University of Alberta, Edmonton, AB T6G 2G1, Canada
e-mail: mli@math.ualberta.ca

A.G. Lim (✉)
Centre for Mathematical Biology, Mathematical Institute, University of Oxford, 24-29 St Giles', Oxford OX1 3LB, UK
e-mail: aaron.lim@maths.ox.ac.uk

individuals remains as asymptomatic carriers (ACs) throughout their lifetime, while approximately 0.1–4% will develop HAM/TSP or ATL (Proietti et al. 2005).

Host immune responses specific to HTLV-I are associated with the activation and clonal expansion of anti-HTLV-I CD8$^+$ cytotoxic T-lymphocytes (CTLs), and such CTLs are typically abundant in the peripheral blood of infected hosts, both ACs and HAM/TSP patients (Asquith et al. 2005; Bangham et al. 2009). A traditional theory for HTLV-I maintenance is that infected cells are almost exclusively latent, escaping CTL-induced lysis by effectively remaining 'invisible' to host immune responses, and the proviral load is maintained principally by normal homeostatic mitotic division of CD4$^+$ helper T-cells, the primary targets of HTLV-I (Mortreux et al. 2003; Wattel et al. 1996). Such a mechanism does not adequately justify the high frequencies of circulating anti-HTLV-I CD8$^+$ CTLs found in the peripheral blood, which require antigenic stimulation from transcriptionally active proviral cells in order to proliferate. These HTLV-I-specific CTLs have been shown to be chronically activated in infected individuals, suggesting that they have recently been exposed to antigen in vivo (Asquith et al. 2005; Bangham et al. 2009). The high proviral loads often observed cannot be maintained solely by normal homeostatic mitosis of CD4$^+$ helper T-cells; selective proliferation of provirus-containing cells must be involved. A new hypothesis has been proposed in Asquith and Bangham (2007, 2008) that focuses on the dynamic interaction between transcriptional latency of proviral cells and infected target cell activation corresponding to either suppression or expression of viral antigens. This hypothesis suggests a way in which HTLV-I-infected individuals can display elevated proviral loads while maintaining a persistently activated HTLV-I-specific immune response.

The viral protein Tax is a crucial antigen expressed by cells productively infected by HTLV-I and is involved in activating the transcription of HTLV-I genes and triggering infected T-cell proliferation (Bangham 2000). Proviral cells can be crudely separated into two types, which may be distinguished by the absence or presence of Tax inside the cell due to T-cell latency or T-cell activation: (i) latently infected, or Tax$^-$, target cells are resting CD4$^+$ helper T-cells that contain a provirus and do not express Tax, and (ii) actively infected, or Tax$^+$, target cells are activated provirus-carrying CD4$^+$ helper T-cells that do express Tax. Latently infected cells are transcriptionally silent and do not make new virions, whereas actively infected cells undergo persistent selective replication of the virus, and is hypothesized to be driven by the expression of Tax (Asquith and Bangham 2007, 2008).

Tax expression can be both beneficial and detrimental to the HTLV-I proviral cell. On the one hand, expressing the viral protein is required for cell-to-cell transmission and drives rapid selective clonal expansion of actively infected cells via up-regulation of cellular genes involved in mitosis and down-regulation of cell-cycle checkpoints (Asquith and Bangham 2007, 2008; Mortreux et al. 2003; Wattel et al. 1996). On the other hand, Tax expression simultaneously exposes the proviral cell to immune surveillance as the Tax protein is the dominant antigen recognized by anti-HTLV-I host immune responses, both humoral and cell-mediated (Asquith and Bangham 2007, 2008; Bangham et al. 2009; Wattel et al. 1996). Indeed, lysis of HTLV-I-infected cells by CD8$^+$ CTLs is highly efficient and target Tax$^+$ proviral cells; Tax$^-$ proviral cells evade detection and subsequent destruction (Asquith and Bangham 2007, 2008; Bangham et al. 2009;

Bangham and Osame 2005). Blood samples taken from most HTLV-I-infected individuals consistently show the presence of large, chronically activated Tax-specific CTL responses, suggesting that Tax is continuously being expressed (Asquith and Bangham 2008). Thus, it is plausible that HTLV-I persists in-host not by complete viral latency, but rather by balancing latency with activation. To investigate the outcomes of the dynamic interactions of HTLV-I infection and immune responses, and the overall role played by Tax expression in the persistence of HTLV-I in vivo, we propose and analyze a mathematical model based on the new theoretic hypothesis in Asquith and Bangham (2007, 2008).

2 Formulation of Mathematical Model

To formulate a mathematical model that explores the role of Tax expression in the dynamic interaction between transcriptional latency and viral activation, we compartmentalize the $CD4^+$ T-cell population into three distinct classes. Denote by $x(t)$, $u(t)$, and $y(t)$ the numbers of healthy, latently infected (Tax^-), and actively infected (Tax^+) $CD4^+$ helper T-cells at time t.

It is common to assume that healthy $CD4^+$ helper T-cells are produced in the bone marrow at a constant rate λ and enter the bloodstream (Nowak and May 2000; Perelson 2002). Infectious or horizontal transmission of HTLV-I occurs via direct cell-to-cell contact between an actively infected (Tax^+) and healthy $CD4^+$ helper T-cell (Shiraki et al. 2003), and new incidence is described by a bilinear term βxy, where β is the coefficient of infectious transmissibility (Nelson et al. 2000; Nowak and May 2000). Within 7–10 days after the initial infection, strong adaptive immune responses targeting the Tax protein are established in an attempt to counter-act the infection (Bangham 2000). It is known that the HTLV-I genome displays low genetic sequence variability; infectious transmission is highly error-prone and would result in a genetically diverse pool of infected target cells (Asquith and Bangham 2007; Mortreux et al. 2003; Wattel et al. 1996). It is assumed that only a small fraction σ, where $\sigma \in (0, 1)$ and $\sigma \ll 1$, of newly infected Tax^+ target cells via infectious transmission survive and silence Tax expression, by mechanisms that are not yet understood (Asquith and Bangham 2008; Mortreux et al. 2003; Wattel et al. 1996).

A small proportion τ of latently infected (Tax^-) $CD4^+$ T-cells spontaneously express the viral Tax protein and become actively infected (Tax^+) (Asquith and Bangham 2008). Mitotic or vertical transmission of HTLV-I involving selective clonal expansion of these Tax-expressing proviral $CD4^+$ T-cells occurs at a rate r and is modelled by a logistic growth term. Although mitosis is a natural process that occurs in all $CD4^+$ T-cells, normal homeostatic proliferation occurs at a much slower rate than that of selective mitotic division of Tax^+ proviral cells. To avoid unnecessarily complicating the mathematical analysis, we ignore the effects of passive proliferation of the healthy and latently infected target cell populations. Newly infected cells via mitotic transmission risk elimination by CTL-mediated lysis. The genetic stability of HTLV-I along with the frequently observed high proviral loads in infected hosts imply that a significant proportion ϵ, where $\epsilon \in (0, 1)$ and $\epsilon \approx 1$, survives and hides
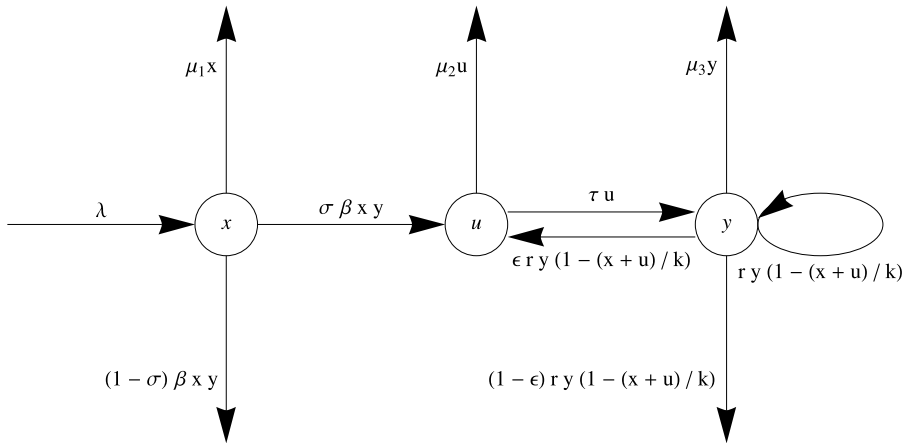
Fig. 1 Transfer diagram describing the infection dynamics of HTLV-I in vivo

Tax expression, thereby contributing to the latently infected target cell compartment. Since the vast majority of proviral cells are transcriptionally latent then at any given time t, $y(t) \ll u(t)$, and it is biologically plausible to use the form $ry(1 - \frac{x+u}{k})$, instead of $ry(1 - \frac{x+u+y}{k})$, to describe the vertical transmission of HTLV-I, where k is the CD4$^+$ helper T-cell carrying capacity. We assume that all target cell populations under consideration are removed from the system by natural cell death at a rate proportional to their numbers. The removal rates of uninfected, latently infected, and actively infected CD4$^+$ helper T-cells are denoted by μ_1, μ_2, μ_3, respectively. All parameters are assumed to be positive. A transfer diagram for the described interactions is shown in Fig. 1.

Based on our assumptions, we derive the following system of ordinary differential equations:

$$
\begin{aligned}
x' &= \lambda - \beta xy - \mu_1 x, \\
u' &= \sigma \beta xy + \epsilon r y \left(1 - \frac{x+u}{k} \right) - (\tau + \mu_2)u, \\
y' &= \tau u - \mu_3 y.
\end{aligned}
\tag{1}
$$

Mathematical models that take into account both infectious and mitotic routes of viral transmission as well as the role of HTLV-I-specific immune responses have been constructed by Gómez-Acevedo and Li (2005) and Wodarz et al. (1999). Model (1) extends these earlier models by incorporating the role of the viral protein Tax during the course of infection, whose expression confers both advantages and disadvantages to the proviral cell. In our mathematical model (1), the differentiation of the infected cell class into two pools, latent and active, illustrates for the first time a highly dynamic interaction between viral expression and transcriptional latency that is critical to the persistence of HTLV-I in vivo.

3 Equilibria, Local Stability, and Backward Bifurcation

For the mathematical analysis of model (1), we first derive upper bounds for the T-cell populations to find a biologically relevant region for which our model is well-posed. The result is stated in Theorem 3.1 and the proof is given in Appendix B. Since the parameter k denotes the carrying capacity of CD4$^+$ helper T-cells in the peripheral blood, it is natural to expect that $x + u + y \leq k$ for all time. For this to hold, we need to make the following compatibility condition:

$$(A_0) \quad \frac{\lambda}{\tilde{\mu}} \leq k,$$

where $\tilde{\mu} = \min\{\mu_1, \mu_2\}$. Denote by $\mathbb{R}^3_+$ the closed positive orthant of $\mathbb{R}^3$, and let

$$\Gamma := \left\{ (x, u, y) \in \mathbb{R}^3_+ : x \leq \frac{\lambda}{\mu_1}, \ x + u \leq k, \ y \leq \frac{\tau}{\mu_3} k \right\}. \tag{2}$$

Theorem 3.1 *The set Γ is positively invariant with respect to model (1). All solutions of model (1) are bounded for $t \geq 0$ and eventually enter Γ.*

Theorem 3.1 defines the set Γ as a feasible region on which the dynamics may be analyzed. The global dynamics of model (1) are determined by the basic reproduction number for viral infection,

$$R_0 = \frac{\sigma \beta \tau x_0}{\mu_3(\tau + \mu_2)} + \frac{\epsilon r \tau}{\mu_3(\tau + \mu_2)} \left(1 - \frac{x_0}{k}\right) > 0, \quad \text{where } x_0 = \frac{\lambda}{\mu_1}. \tag{3}$$

Biologically, R_0 represents the average number of secondary infected cells produced from a single actively infected cell over its lifetime. The first term in the sum of R_0 represents secondary infections through horizontal (infectious) transmission, while the second term represents secondary infections from vertical (mitotic) transmission.

Define

$$\sigma_0 = \frac{\epsilon r}{k\beta} - \frac{\epsilon r - \frac{\mu_3}{\tau}(\tau + \mu_2)}{2\beta x_0} \left[\frac{k\beta\tau(\epsilon r - \frac{\mu_3}{\tau}(\tau + \mu_2))}{2\epsilon r \mu_1 \mu_3} + 1 \right], \tag{4}$$

and

$$\bar{\sigma} = \frac{\epsilon r}{k\beta} - \frac{1}{\beta x_0}\left(\epsilon r - \frac{\mu_3}{\tau}(\tau + \mu_2)\right). \tag{5}$$

Throughout this paper, we make the following mild mathematical assumptions:

$$(A_1) \quad \epsilon r - \frac{\mu_3}{\tau}(\tau + \mu_2) > 0,$$

$$(A_2) \quad \sigma \beta < \frac{\epsilon r}{k},$$

$$(A_3) \quad 0 < \sigma_0 < \bar{\sigma}.$$

If we consider $R_0 = R_0(\sigma)$ as a function of σ, then $R_0(\sigma)$ is increasing and $\bar{\sigma}$ satisfies $R_0(\bar{\sigma}) = 1$. Hence, Assumption (A_3) is equivalent to $R_0(\sigma_0) < R_0(\bar{\sigma}) = 1$. Assumption (A_1) requires that the net effect of infected T-cell activation and Tax expression is stronger than transcriptional latency. Assumption (A_2) implies that infectious transmission has less of an impact in maintaining the proviral load than mitotic transmission. Assumption (A_3) states that both chronic infection and viral clearance are theoretically possible outcomes of the infection.

There are two types of equilibria for model (1): the infection-free equilibrium $P_0 = (x_0, 0, 0)$ corresponding to a healthy individual, and chronic-infection equilibria $\bar{P} = (\bar{x}, \bar{u}, \bar{y})$, where $\bar{x}, \bar{u}, \bar{y} > 0$ satisfy

$$0 = \lambda - \beta \bar{x} \bar{y} - \mu_1 \bar{x}, \tag{6}$$

$$0 = \sigma \beta \bar{x} \bar{y} + \epsilon r \bar{y} \left(1 - \frac{\bar{x} + \bar{u}}{k} \right) - (\tau + \mu_2) \bar{u}, \tag{7}$$

$$0 = \tau \bar{u} - \mu_3 \bar{y}. \tag{8}$$

From (7)–(8), we find that

$$\bar{y} = \frac{k\tau}{\epsilon r \mu_3} \left[\left(\sigma \beta - \frac{\epsilon r}{k} \right) \bar{x} + \epsilon r - \frac{\mu_3}{\tau}(\tau + \mu_2) \right] \quad \text{and} \quad \bar{u} = \frac{\mu_3}{\tau} \bar{y}. \tag{9}$$

Substitution into (6) then yields

$$\lambda - \mu_1 \bar{x} = \frac{k\beta\tau}{\epsilon r \mu_3} \bar{x} \left[\left(\sigma \beta - \frac{\epsilon r}{k} \right) \bar{x} + \epsilon r - \frac{\mu_3}{\tau}(\tau + \mu_2) \right].$$

Define

$$f_1(x) = \lambda - \mu_1 x,$$
$$f_2(x) = \frac{k\beta\tau}{\epsilon r \mu_3} x \left[\left(\sigma \beta - \frac{\epsilon r}{k} \right) x + \epsilon r - \frac{\mu_3}{\tau}(\tau + \mu_2) \right]. \tag{10}$$

The x-coordinates of chronic-infection equilibria, if they occur, are the intersection points of the line f_1 with the parabola f_2; see Fig. 2. Observe that Assumptions (A_1) and (A_2) are precisely the requirements that $f_2'(0) > 0$ and $f_2''(x) < 0$, respectively. Note that both f_1 and f_2 have a single positive root. Assumption (A_3) ensures that for some positive value of the parameter σ, the height of the vertex of the concave parabola f_2 lies above the height of the corresponding point on the straight line f_1, and a range for σ exists, in which the number of chronic-infection equilibria goes from zero to two as σ increases.

We summarize the results for the existence of equilibria in the following theorem.

Theorem 3.2 *Assume that (A_1)–(A_3) hold. Then*

(1) *the infection-free equilibrium $P_0 = (x_0, 0, 0)$, where $x_0 = \frac{\lambda}{\mu_1}$, always exists in $\bar{\Gamma}$. Moreover, if $0 < R_0 < R_0(\sigma_0)$, then P_0 is the only equilibrium in $\bar{\Gamma}$;*
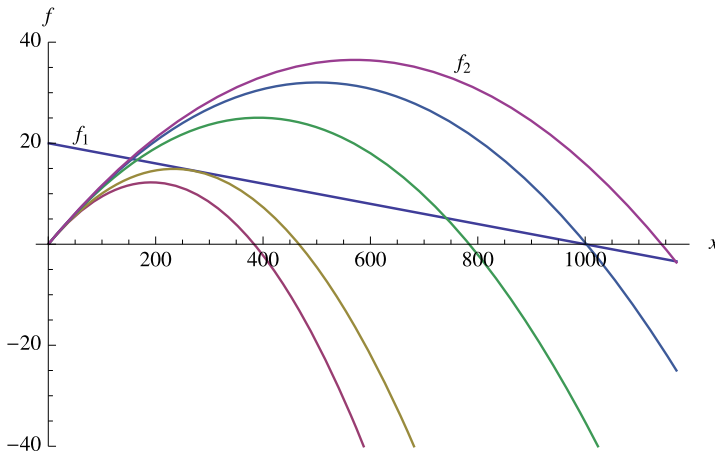
Fig. 2 Graphs of the *straight line* f_1 and the *concave parabola* f_2 for several values of the parameter σ. As σ varies, the two graphs may have zero, one, or two intersection points. All parameter values are selected in the ranges shown in Table 1

(2) *when $R_0(\sigma_0) < R_0 < 1$, there exist three equilibria, P_0 on the boundary $\partial\Gamma$ and two distinct chronic-infection equilibria $P_1 = (x_1, u_1, y_1)$ and $P_2 = (x_2, u_2, y_2)$, with $x_1 < x_2$. Furthermore, $f_1'(x_1) < f_2'(x_1)$ and $f_1'(x_2) > f_2'(x_2)$;*

(3) *when $R_0 > 1$, there exist exactly two equilibria, P_0 on $\partial\Gamma$ and a unique chronic-infection equilibrium $P_1 = (\bar{x}, \bar{u}, \bar{y})$, whose x-coordinate satisfies $f_1'(\bar{x}) < f_2'(\bar{x})$.*

Next, the local stability of equilibria is examined and the results are stated in Theorems 3.3 and 3.4. The proofs may be found in Appendix B. We first establish the basic reproduction number for viral infection R_0 as a threshold parameter characterizing the local stability of the infection-free equilibrium P_0.

Theorem 3.3

(i) *When $R_0 < 1$, the infection-free equilibrium P_0 is always locally asymptotically stable in the feasible region Γ.*

(ii) *When $R_0 > 1$, P_0 is unstable. More specifically, P_0 is a saddle with $\dim W_{\text{loc}}^s(P_0) = 2$ and $\dim W_{\text{loc}}^u(P_0) = 1$, where $W_{\text{loc}}^s(P_0)$, $W_{\text{loc}}^u(P_0)$ denote the local stable and unstable manifolds of P_0, respectively.*

Theorem 3.4 *Assume that (A_1)–(A_3) hold. Then*

(i) *when $R_0(\sigma_0) < R_0 < 1$, the chronic-infection equilibrium P_1 is locally asymptotically stable whereas P_2 is unstable. Moreover, the local stable manifold $W_{\text{loc}}^s(P_2)$ of P_2 is two-dimensional;*

(ii) *when $R_0 > 1$, the unique chronic-infection equilibrium P_1 is locally asymptotically stable.*

Theorems 3.2–3.4 establish the existence of a backward bifurcation leading to a region of bi-stability. There is an open range of the parameter $\sigma \in (\sigma_0, \bar{\sigma})$, such that
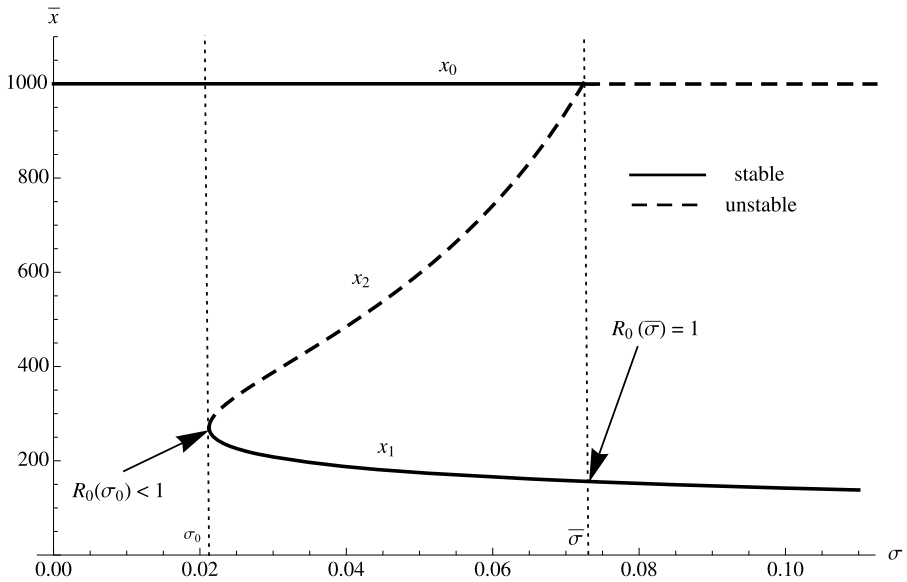
Fig. 3 Backward bifurcation and bi-stability of equilibria with respect to the parameter σ. Parameter values are selected from the ranges as in Table 1: $\lambda = 20$, $\beta = 0.001$, $\epsilon = 0.9$, $\tau = 0.01$, $r = 0.15$, $k = 1150$, $\mu_1 = 0.02$, $\mu_2 = 0.02$, $\mu_3 = 0.03$

the infection-free equilibrium P_0 and a chronic-infection equilibrium P_1 co-exist and are both stable. The bifurcation diagram is shown in Fig. 3. Backward bifurcation is also shown to occur in a model for HTLV-I infection in Gómez-Acevedo and Li (2005), suggesting that such a phenomenon is intrinsic to the dynamics of HTLV-I. Challenges to effective treatment strategies to HTLV-I infection arising from a backward bifurcation due to bi-stability and hysteresis effects are examined in Gómez-Acevedo and Li (2005). In Sect. 4, we will further discuss biological implications of a backward bifurcation with respect to viral infection.

4 Global Dynamics

We first show that model (1) is a cooperative system.

Proposition 4.1 *Model* (1) *is cooperative with respect to the partial ordering defined by the orthant*

$$K = \left\{ (x, u, y) \in \mathbb{R}^3 : x \leq 0, u \geq 0, y \geq 0 \right\}.$$

Furthermore, system (1) *is irreducible in* $\overset{\circ}{\Gamma}$.

Proof The Jacobian matrix for model (1) is

$$J(x, u, y) = \begin{bmatrix} -\beta y - \mu_1 & 0 & -\beta x \\ (\sigma\beta - \frac{\epsilon r}{k})y & -\frac{\epsilon r}{k}y - \tau - \mu_2 & \sigma\beta x + \epsilon r(1 - \frac{x+u}{k}) \\ 0 & \tau & -\mu_3 \end{bmatrix}.$$

Assumption (A_0) implies that $x + u \leq k$, and thus $1 - (x+u)/k \geq 0$. Also, Assumption (A_2) implies $(\sigma\beta - \epsilon r/k)y \leq 0$, and the matrix $J(x,u,y)$ is irreducible if $y > 0$. Choose $Q = \mathrm{diag}(-1,1,1)$. Then QJQ^{-1} has non-negative off-diagonal elements. The first claim follows from Lemma 2.1 in Smith (1998). $\qquad\square$

Applying the theory of monotone dynamical systems (Hirsch 1982; Smith 1995), we obtain the following global stability results.

Theorem 4.1 (Global Stability when P_0 is the Only Equilibrium in Γ) *When $0 < R_0 < R_0(\sigma_0)$, the infection-free equilibrium P_0 is the only equilibrium in $\bar{\Gamma}$ and it is globally asymptotically stable.*

Proof The set $\mathring{\Gamma} \cup \{P_0\}$ is convex and positively invariant, and contains a unique equilibrium P_0. Applying Proposition 4.1 in $\mathring{\Gamma} \cup \{P_0\}$ establishes the global stability of P_0 in the interior $\mathring{\Gamma}$ of Γ [Smith 1995, Theorem 3.1]. On the boundary of Γ, the direction of the vector field for model (1) indicates that solutions starting on $\partial\Gamma$ either enter $\mathring{\Gamma}$ and subsequently converge to P_0, or remain on the positively invariant x-axis and converge to P_0 along the x-axis. This establishes the global stability of P_0 in the closure $\bar{\Gamma}$ of Γ. $\qquad\square$

A similar argument may be used to establish the global stability when a unique chronic-infection equilibrium exists in the interior $\mathring{\Gamma}$ of Γ.

Theorem 4.2 (Global Stability of the Unique Chronic-Infection Equilibrium when $R_0 > 1$) *Assume that $R_0 > 1$. Then, there exists a unique chronic-infection equilibrium P_1 and it is globally asymptotically stable in $\mathring{\Gamma}$.*

If $\sigma_0 = \bar{\sigma}$, or equivalently $R_0(\sigma_0) = 1$, then the range of σ for backward bifurcation and bi-stability disappears and the standard forward bifurcation is observed. In this case, Theorems 4.1 and 4.2 together establish the global behavior of solutions to model (1), and the basic reproduction number for viral infection R_0 acts as a sharp threshold parameter completely characterizing the global dynamics of model (1).

Next, we establish the global dynamics when backward bifurcation occurs, namely when $\sigma_0 < \bar{\sigma}$. Because of multi-stability, the proof for Theorems 4.1 and 4.2 does not apply. It is known that the Poincaré–Bendixson theorem holds for three-dimensional cooperative systems (Hirsch 1982; Smith 1995). Since model (1) is cooperative, it may only admit unstable periodic trajectories when multiple equilibria exist in $\mathring{\Gamma}$. Using a result of Muldowney [1990, Theorem 4.2], we prove that any non-constant periodic solution of model (1), if it exists, is orbitally asymptotically stable with asymptotic phase. This allows us to establish the non-existence of periodic orbits in the feasible region Γ. The proofs of the following two theorems are given in Appendix B.

Theorem 4.3 (Non-existence of Closed Orbits in Γ) *There cannot exist any non-constant periodic solutions of model (1) in Γ provided*

$$(A_4) \quad \frac{\epsilon r}{k} < 2\sigma\beta.$$

Biologically, Assumption (A_4) requires that both infectious and mitotic transmission of HTLV-I are important for the infection.

Theorem 4.4 (Global Dynamics when Bi-stability Occurs) *Assume that (A_1)–(A_3) hold. When $R_0(\sigma_0) < R_0 < 1$, there exist three equilibria in $\bar{\Gamma}$: the infection-free equilibrium P_0 on the boundary $\partial\Gamma$, along with two distinct chronic-infection equilibria P_1 and P_2 in the interior $\mathring{\Gamma}$. Under Assumption (A_4), both P_0 and P_1 are attractors whose basins of attraction are separated by the two-dimensional stable manifold of the saddle point P_2.*

Our main theoretical results give rise to the following biological implications.

(a) If $0 < R_0 < R_0(\sigma_0)$, an infected individual can elicit a strong immune response against the virus and the infection is cleared. Even with a high initial viral dosage, chronic infection does not occur.
(b) If $R_0 > 1$, the individual elicits a weak immune response against the virus. Such a scenario may occur in individuals whose circulating CTLs or antibodies have poor recognition of HTLV-I epitopes, or those who are immuno-compromised. Even with a small initial viral dosage, chronic infection ensues.
(c) If $R_0(\sigma_0) < R_0 < 1$, backward bifurcation and bi-stability are present. In this case, the outcome of the infection, whether it is cleared or becomes chronic, is dependent on the initial viral dosage at the onset of the infection: a low initial viral dosage can be cleared by the host, whereas a high enough initial viral dosage leads to chronic infection.

5 Numerical Investigations

In this section, we investigate several important aspects of model (1) numerically. We will use parameter values that have been estimated using both experimental and theoretical methods in studies of CD4^{+} lymphocyte kinetics by Asquith et al. (2007), Kirschner and Webb (1996), and Nelson et al. (2000). In particular, the rate of production of healthy CD4^{+} helper T-cells from the bone marrow falls in the range of 10–25 cells/mm³/day (Kirschner and Webb 1996). As infection by HTLV-I only causes minor detriment to T-cell functionality (Asquith and Bangham 2007), it is expected that all three populations of target cells considered in our model display natural death rates similar to that of healthy target cells, between 0.01–0.05 day^{−1} (Kirschner and Webb 1996; Nelson et al. 2000). The rate of rapid Tax-driven selective mitosis r lies in the range 0.04–0.4 per day, which is in the same order of magnitude as the one proposed in Kirschner and Webb (1996). In the absence of infection, the normal CD4^{+} helper T-cell count averages 1000 cells/mm³, and we consider a target cell carrying capacity of 1150 cells/mm³. Using a scaling relation of Perelson (1989), $\beta k \approx 1$, and when the time unit is per day, we determine values for the coefficient of infectious transmissibility β to be in the order of 10^{-3} mm³/cell/day. Asquith et al. (2007) have quantified the rate τ of expression of Tax in proviral cells to be between 0.03–3% per day. The biological meaning of the parameters as well as the relevant ranges in which the parameters lie are summarized in Table 1. It is easily verified that when

Table 1 Biologically relevant parameter values

Parameter	Range or value	Biological meaning
λ	10–25 cells/mm^3/day	Rate of production of target cells (CD4$^+$ helper T-cells)
β	0.0005–0.003 mm^3/cell/day	Coefficient of infectious transmissibility
r	0.04–0.4 day^{-1}	Rate of Tax-driven selective proliferation of actively infected target cells
k	1150 cells/mm^3	Carrying capacity of target cells
σ	0–1	Fraction of infected target cells from infectious transmission surviving immune responses
ϵ	0–1	Fraction of infected target cells from mitotic transmission surviving immune responses
τ	0.0003–0.03 day^{-1}	Rate of spontaneous Tax expression
μ_1	0.01–0.05 day^{-1}	Natural death rate of healthy target cells
μ_2	0.01–0.05 day^{-1}	Natural death rate of latently infected target cells
μ_3	0.01–0.05 day^{-1}	Natural death rate of actively infected target cells

parameter values are selected from these ranges, the assumptions and theoretical results observed in Sects. 3 and 4 are valid, thus the behaviors of solutions to model (1) stated in these sections are plausible for HTLV-I infection.

5.1 Establishment of Proviral Load and Viral Persistence in Latently Infected Cells

The proviral load of a chronically infected individual at equilibrium is commonly expressed as a proportion or percentage of the total number of CD4$^+$ helper T-cells. Specifically,

$$\text{Equilibrium Proviral Load} = \frac{\text{number of infected cells}}{\text{total number of cells}}$$
$$= \frac{\bar{u} + \bar{y}}{\bar{x} + \bar{u} + \bar{y}}. \tag{11}$$

Numerical simulation of model (1) as in Fig. 4 shows that the proviral load at equilibrium is 77% CD4$^+$. Our model agrees with the common experimental observation that an HTLV-I-infected person may harbor a high proviral load (Bangham 2000; Mortreux et al. 2003; Wattel et al. 1996).

The proportion of infected cells that are latent in an infected individual is

$$\text{Proportion of Latently Infected Cells}$$
$$= \frac{\text{number of Tax}^- \text{ infected cells}}{\text{total number of infected cells}} = \frac{\bar{u}}{\bar{u} + \bar{y}}. \tag{12}$$
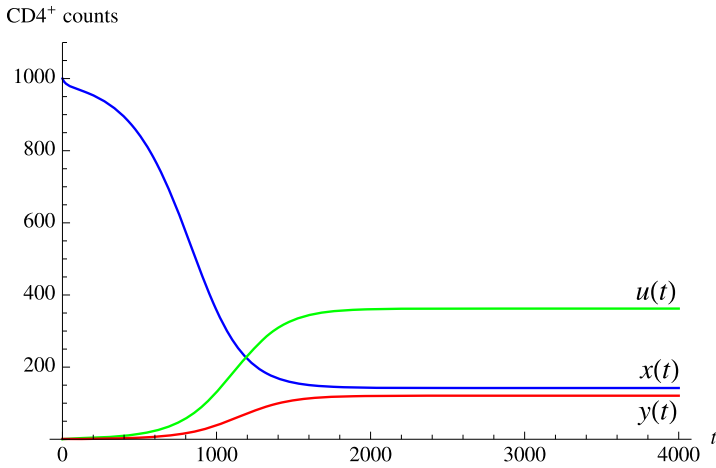
Fig. 4 Chronic infection by HTLV-I. The level of healthy target cells $x(t)$, latently infected target cells $u(t)$, and actively infected target cells $y(t)$ are shown over the course of approximately 11 years from the initial infection. The parameter values are: $\lambda = 20$, $\beta = 0.001$, $\sigma = 0.1$, $\epsilon = 0.9$, $\tau = 0.01$, $r = 0.15$, $k = 1150$, $\mu_1 = 0.02$, $\mu_2 = 0.02$, $\mu_3 = 0.03$

In Fig. 4, 75% of the equilibrium proviral load is comprised of latently infected cells. Our simulations agree with the experimental observation that the vast majority of proviral cells are transcriptionally latent (Asquith and Bangham 2007, 2008).

5.2 Tax Expression is Positively Correlated with Proviral Load

As shown in Fig. 5, the rate of spontaneous Tax expression τ displays a positive correlation with the equilibrium proviral load during chronic infection by HTLV-I. This observation suggests that the net effect of increased Tax expression, which exposes the proviral cell to immune surveillance and raises its risk of elimination by CTLs, is to increase rather than decrease the proviral load. The benefits conferred by T-cell activation, such as infectious transmission and rapid mitotic transmission, allow the provirus to replicate faster than it is being destroyed. The proviral load should then be expected to increase as the surviving proportion of newly infected cells, either through horizontal or vertical transmission, subsequently hide viral protein expression and become latent. This conclusion agrees with theoretical studies in Asquith and Bangham (2007, 2008).

5.3 Tax Expression Drives Chronic Infection and Promotes Bi-stability

We make two observations regarding the effect of Tax expression in determining whether the infection becomes chronic or dies out. First, a simple computation yields

$$\frac{\partial R_0}{\partial \tau} = \frac{\mu_2}{\mu_3(\tau + \mu_2)^2}\left(\sigma\beta x_0 + \epsilon r\left(1 - \frac{x_0}{k}\right)\right) > 0,$$

that is, an increase in the rate of spontaneous Tax expression increases the possibility of viral persistence.
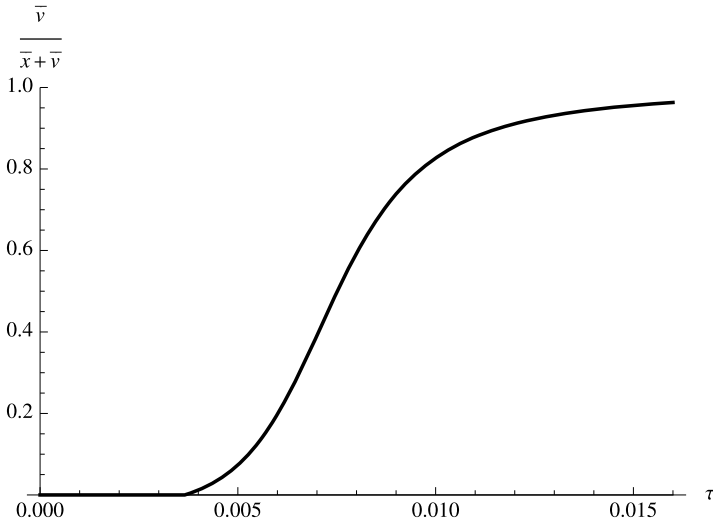
Fig. 5 The rate of spontaneous Tax expression and the equilibrium proviral load display a positive correlation. Parameter values are: $\lambda = 20$, $\beta = 0.003$, $\sigma = 0.06$, $\epsilon = 0.9$, $r = 0.12$, $k = 1150$, $\mu_1 = 0.02$, $\mu_2 = 0.02$, $\mu_3 = 0.03$
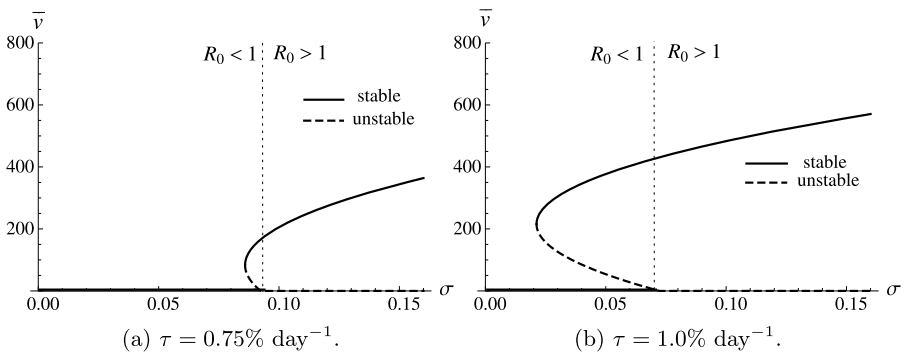
Fig. 6 Tax expression increases the range for which backward bifurcation and bi-stability occur. Parameter values are: $\lambda = 20$, $\beta = 0.001$, $\epsilon = 0.9$, $r = 0.15$, $k = 1150$, $\mu_1 = 0.02$, $\mu_2 = 0.02$, $\mu_3 = 0.03$

Second, numerical simulations indicate that increasing τ also increases the range for which backward bifurcation and bi-stability occur, as illustrated in Fig. 6. A broader range for the presence of bi-stability means that (i) newly infected individuals would have a higher probability of lying in the basin of attraction of the stable chronic-infection equilibrium, and (ii) a smaller initial viral dosage would be sufficient to cause chronic infection. An increased rate of Tax expression is therefore seen to be a factor that drives the system towards chronic infection.

(a) $\tau = 0.42\%$ day^{-1}. Clears infection in about 2 years.

(b) $\tau = 0.84\%$ day^{-1}. Takes approximately 15 years to clear infection.

(c) $\tau = 1.00\%$ day^{-1}, $\frac{\bar{v}}{\bar{x}+\bar{v}} = 71\%$ CD4$^+$. Takes over 12 years to reach chronic infection steady state.

(d) $\tau = 1.42\%$ day^{-1}, $\frac{\bar{v}}{\bar{x}+\bar{v}} = 90\%$ CD4$^+$. Submits to infection in less than 2 years with increased proviral load.
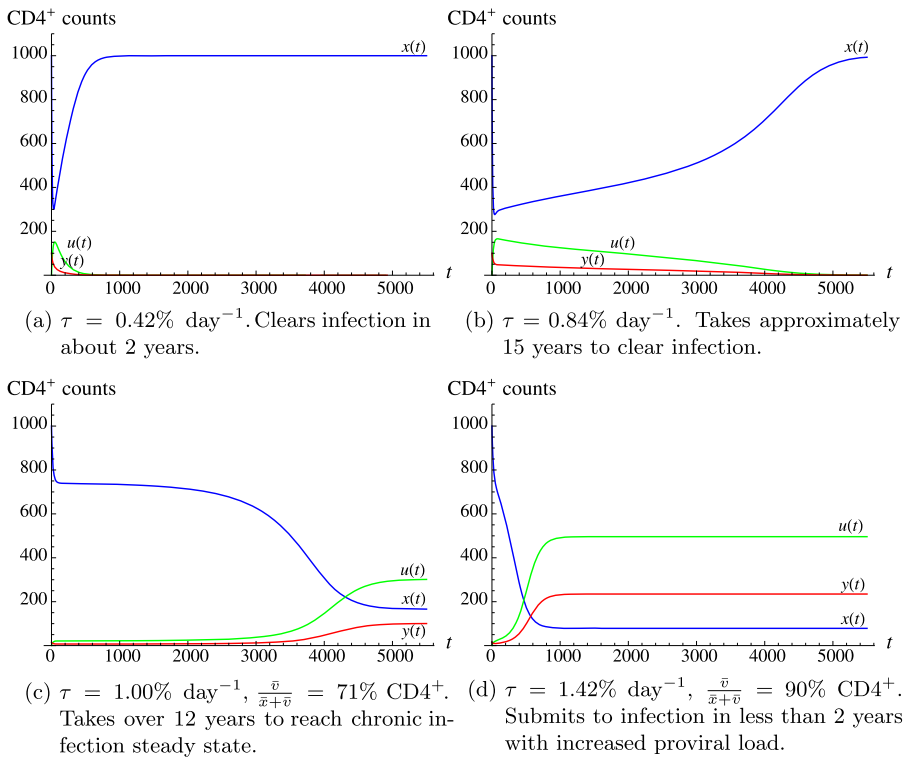
Fig. 7 Time series simulations demonstrating the impact of Tax expression on the duration of time required for an individual to settle at equilibrium. (**a**)–(**b**) Increasing the value of τ increases the time needed to clear HTLV-I. (**c**)–(**d**) The result of increased Tax expression is a decreased time to settle at the chronic infection steady state. Parameter values are: $\lambda = 20$, $\beta = 0.001$, $\sigma = 0.06$, $\epsilon = 0.9$, $r = 0.15$, $k = 1150$, $\mu_1 = 0.02$, $\mu_2 = 0.02$, $\mu_3 = 0.03$

5.4 Tax Expression Affects Time to Reach Chronic-Infection Equilibrium

The rate of expression of viral proteins also has a strong impact on the length of time it takes an individual to reach steady state. Time series plots demonstrating the possible situations are shown in Fig. 7. In Figs. 7(a)–(b), a slight increase in Tax expression significantly increases the time for complete clearance of the virus and for the level of healthy CD4$^+$ helper T-cells to return to normal. During this extended period of time, a lower CD4$^+$ helper T-cell count could reduce overall immune functionality and leave the host more susceptible to invading pathogens including bacterial or other viral infections. In Figs. 7(c)–(d), a small increase in Tax expression not only increases the proviral load at equilibrium, it also reduces considerably the length of time required to reach the chronic infection steady state. It is possible that the sudden sharp decline in healthy CD4$^+$ helper T-cell counts in chronically infected individuals induced by a high continuous rate of viral protein expression is a crucial factor in the pathogenesis of the inflammatory disease HAM/TSP.

6 Discussion

In this paper, we have developed a mathematical model based on a new hypothesis in Asquith and Bangham (2007, 2008) for the persistence of HTLV-I infection in vivo, focusing on the role of Tax expression in viral replication, transmission, and maintenance. The proposed mechanism of viral infection considers a highly dynamic interaction among three compartments of target cells of the virus: healthy, latently infected, and actively infected CD4$^+$ helper T-cells. The differentiation between two pools of infected target cells and the relationship between them are key features of our model and represent important aspects of realistic HTLV-I infection that have not been considered in previous mathematical models of HTLV-I. Our findings demonstrate that a balance between transcriptional latency and activation of proviral cells offers opportunities for HTLV-I to evade destruction by human immune responses while establishing high proviral loads, and that the rate τ of spontaneous expression of the viral protein Tax has a substantial impact on the outcome of HTLV-I infection.

The proportion of the equilibrium proviral load consisting of actively infected target cells depends only on the parameters τ and μ_3, and is equal to $\frac{\tau}{\tau+\mu_3}$. Direct calculation shows that

$$\frac{\partial}{\partial\tau}\left(\frac{\tau}{\tau+\mu_3}\right) = \frac{\mu_3}{(\tau+\mu_3)^2} > 0;$$

that is, a higher rate of Tax expression increases the Tax$^+$ proportion of the proviral load, which in turn stimulates faster proliferation of anti-Tax HTLV-I-specific CTLs. The cytotoxic effects of CTLs have been suggested to be the underlying cause of the tissue damage in the central nervous system leading to the development of HAM/TSP (Asquith et al. 2005; Bangham 2000; Mosley and Bangham 2009). Indeed, a higher rate of Tax expression has been experimentally shown to be associated with a greater risk of developing HAM/TSP (Asquith and Bangham 2007). Our conclusion supports a new postulate in Mosley and Bangham (2009) for HAM/TSP pathogenesis. Our conclusion also helps to rectify conflicting arguments that the proviral load should play an important part in determining disease status yet its magnitude is neither necessary nor sufficient to cause HAM/TSP (Asquith and Bangham 2007; Mosley and Bangham 2009).

Model (1) incorporates anti-HTLV-I immune responses implicitly as in Gómez-Acevedo and Li (2005) by including the parameters σ and ϵ representing fractions of newly infected target cells that survive elimination: stronger immune responses correspond to lower values of σ, ϵ; weaker immune responses correspond to higher values of σ, ϵ. As the primary focus of our model is to illuminate the particular role of Tax expression in HTLV-I persistence, an explicit incorporation of the HTLV-I-specific immune response via a compartment of CD8$^+$ CTLs would greatly complicate the mathematical analysis and make it difficult to draw clear conclusions from the analysis. Nevertheless, the CTL response is an integral part of HTLV-I infection and persistence, and is believed to be directly related to the development of HAM/TSP. It is necessary to include a separate CTL compartment in future modelling investigations.

It is known that Tax, though immuno-dominant, is not the only viral protein recognized by HTLV-I-specific CTLs (Bangham et al. 2009; Bangham and Osame 2005).

Recent research evidence shows that a different HTLV-I gene product, HTLV-I basic leucine zipper factor (HBZ), is also a critical target of the CTL response, and may play an important role in determining the proviral load and risk of HTLV-I-related diseases (Boxus and Willems 2009; Matsuoka and Green 2009; Saito et al. 2009). Further modelling studies incorporating the role of HBZ are needed. Another crude approximation used in our model is the partition of infected CD4$^+$ helper T-cells into Tax$^+$ and Tax$^-$ groups. It is becoming increasingly clear that the expression of the provirus in each distinct HTLV-I-infected T-cell clone is likely to be different, and depends on the integration site in the host genome (Bangham et al. 2009; Meekings et al. 2008). As a result, there may be a continuum of proviral expression and a varying degree of susceptibility to CTL-mediated lysis. Improved models incorporating this structure need to be further investigated to gain a more in-depth understanding of HTLV-I dynamics in vivo.

Appendix A: Second Additive Compound Systems

Let A denote a linear operator on $\mathbb{R}^n$ as well as its matrix representation with respect to the standard canonical basis of $\mathbb{R}^n$. Denote by $\bigwedge^2 \mathbb{R}^n$ the exterior product of $\mathbb{R}^n$ consisting of exterior products $v_1 \wedge v_2$ of two vectors v_1, v_2 in $\mathbb{R}^n$. The linear operator A, along with its standard basis of $\mathbb{R}^n$, induces a linear operator $A^{[2]}$ with corresponding canonical basis of $\bigwedge^2 \mathbb{R}^n$. Its matrix representation with respect to the canonical basis in $\bigwedge^2 \mathbb{R}^n$ is called the *second additive compound matrix of A* (Fiedler 1974; Muldowney 1990). It satisfies the property $(A + B)^{[2]} = A^{[2]} + B^{[2]}$ for any two $n \times n$ matrices A and B. The second additive compound matrix of $A = [a_{ij}]$ when $n = 3$ is given below by

$$A^{[2]} = \begin{bmatrix} a_{11} + a_{22} & a_{23} & -a_{13} \\ a_{32} & a_{11} + a_{33} & a_{12} \\ -a_{31} & a_{21} & a_{22} + a_{33} \end{bmatrix}. \tag{13}$$

Let $f : D \to \mathbb{R}^n$ be a continuously differentiable function defined on an open set $D \subset \mathbb{R}^n$ and consider the autonomous system of ordinary differential equations

$$x' = f(x), \quad x \in D. \tag{14}$$

The *kth compound system* associated to the non-linear autonomous system of ordinary differential equations (14) is a system of linear equations

$$z' = \frac{\partial f}{\partial x}^{[2]} z, \tag{15}$$

where $\frac{\partial f}{\partial x}^{[2]}$ is the second additive compound matrix of the Jacobian matrix, $\frac{\partial f}{\partial x}$, of f.
The following result of Muldowney (1990) is critical to the proof of Theorem 4.3.

Theorem A (Theorem 4.2, Muldowney 1990) *A non-constant periodic solution $x = p(t)$ of system (14) is orbitally asymptotically stable with asymptotic phase if the linear second compound system*

$$z'(t) = \frac{\partial f^{[2]}}{\partial x}(p(t))z(t)$$

is asymptotically stable.

Appendix B: Proofs

Proof of Theorem 3.1 From the first equation of system (1), we obtain $x' \leq \lambda - \mu_1 x$, and this implies that $\limsup_{t \to \infty} x(t) \leq \frac{\lambda}{\mu_1}$. Adding the first two equations of our model yields

$$(x+u)' \leq \lambda + \epsilon r k \left(1 - \frac{x+u}{k}\right) - \tilde{\mu}(x+u),$$

where $\tilde{\mu} = \min\{\mu_1, \mu_2\}$. Therefore, $\limsup_{t \to \infty}(x+u)(t) \leq \frac{\lambda + \epsilon r k}{\epsilon r + \tilde{\mu}} = N$. Finally, if $(x(t), u(t), y(t))$ is a solution of system (1) with $x(0) + u(0) \leq N$, then from the third equation of our model, we obtain

$$y' = \tau u - \mu_3 y \leq \tau N - \mu_3 y,$$

and thus

$$\limsup_{t \to \infty} y(t) \leq \frac{\tau}{\mu_3} N.$$

Using condition (A_0), it can be verified that $N \leq k$, and thus the feasible region for model (1) is

$$\Gamma := \left\{(x, u, y) \in \mathbb{R}^3_+ : x \leq \frac{\lambda}{\mu_1}, \; x + u \leq k, \; y \leq \frac{\tau}{\mu_3} k\right\}.$$

It can be verified that Γ is positively invariant in $\mathbb{R}^3$ and that the model is well-posed. $\qquad\square$

Proof of Theorem 3.3 At the infection-free equilibrium P_0, the Jacobian matrix is

$$J(P_0) = \begin{bmatrix} -\mu_1 & 0 & -\beta x_0 \\ 0 & -\tau - \mu_2 & \sigma \beta x_0 + \epsilon r(1 - \frac{x_0}{k}) \\ 0 & \tau & -\mu_3 \end{bmatrix},$$

whose eigenvalues are

$$\zeta_1 = -\mu_1$$

and

$$\zeta_{2,3} = -\frac{1}{2}(\tau + \mu_2 + \mu_3) \pm \frac{1}{2}\sqrt{(\tau + \mu_2 + \mu_3)^2 + 4\mu_3(\tau + \mu_2)[R_0 - 1]}.$$

Clearly, $\mathrm{Re}(\zeta_1)$, $\mathrm{Re}(\zeta_3) < 0$. The sign of $\mathrm{Re}(\zeta_2)$ depends on R_0. If $R_0 < 1$, $\mathrm{Re}(\zeta_2) < 0$ and P_0 is locally asymptotically stable. If $R_0 > 1$, $\mathrm{Re}(\zeta_2) > 0$ and P_0 is a saddle with $\dim W^s_{\mathrm{loc}}(P_0) = 2$ and $\dim W^u_{\mathrm{loc}}(P_0) = 1$. □

To determine the local stability properties of a chronic-infection equilibrium $\widehat{P} = (\hat{x}, \hat{u}, \hat{y})$, we examine the stability of $J(\widehat{P})$, the Jacobian matrix at $\widehat{P}$. We use the following result by McCluskey and van den Driessche (2004), which is equivalent to the general stability criterion developed by Li and Wang (1998, Theorem 3.1) in the special case when $n = 3$.

Lemma A (Lemma 3, McCluskey and van den Driessche 2004) *Let A be a 3×3 matrix with real entries. If $\mathrm{tr}(A)$, $\det(A)$, and $\det(A^{[2]})$ are all negative, then all of the eigenvalues of A have negative real part.*

Proof of Theorem 3.4 At any chronic-infection equilibrium $\widehat{P} = (\hat{x}, \hat{u}, \hat{y})$, the Jacobian matrix is

$$
J(\widehat{P}) = \begin{bmatrix}
-\beta\hat{y} - \mu_1 & 0 & -\beta\hat{x} \\
(\sigma\beta - \frac{\epsilon r}{k})\hat{y} & -\frac{\epsilon r}{k}\hat{y} - \tau - \mu_2 & \sigma\beta\hat{x} + \epsilon r(1 - \frac{\hat{x}+\hat{u}}{k}) \\
0 & \tau & -\mu_3
\end{bmatrix},
$$

and the second additive compound matrix of J is

$$
J^{[2]}(\widehat{P})
$$
$$
= \begin{bmatrix}
-\beta\hat{y} - \mu_1 - \frac{\epsilon r}{k}\hat{y} - \tau - \mu_2 & \sigma\beta\hat{x} + \epsilon r(1 - \frac{\hat{x}+\hat{u}}{k}) & \beta\hat{x} \\
\tau & -\beta\hat{y} - \mu_1 - \mu_3 & 0 \\
0 & (\sigma\beta - \frac{\epsilon r}{k})\hat{y} & -\frac{\epsilon r}{k}\hat{y} - \tau - \mu_2 - \mu_3
\end{bmatrix}.
$$

From the equilibrium equations (6)–(8), we observe that

$$
\sigma\beta\hat{x} + \epsilon r\left(1 - \frac{\hat{x} + \hat{u}}{k}\right) = \frac{\mu_3}{\tau}(\tau + \mu_2)
$$

and

$$
\hat{y} = \frac{k\tau}{\epsilon r \mu_3}\left[\left(\sigma\beta - \frac{\epsilon r}{k}\right)\hat{x} + \epsilon r - \frac{\mu_3}{\tau}(\tau + \mu_2)\right].
$$

We first compute

$$
\mathrm{tr}\big(J(\widehat{P})\big) = -\beta\hat{y} - \mu_1 - \frac{\epsilon r}{k}\hat{y} - \tau - \mu_2 - \mu_3 < 0,
$$

and

$$
\det\big(J^{[2]}(\widehat{P})\big)
$$
$$
= \det \begin{bmatrix}
-\beta\hat{y} - \mu_1 - \frac{\epsilon r}{k}\hat{y} - \tau - \mu_2 & \frac{\mu_3}{\tau}(\tau + \mu_2) & \beta\hat{x} \\
\tau & -\beta\hat{y} - \mu_1 - \mu_3 & 0 \\
0 & (\sigma\beta - \frac{\epsilon r}{k})\hat{y} & -\frac{\epsilon r}{k}\hat{y} - \tau - \mu_2 - \mu_3
\end{bmatrix}
$$

$$
= -\left(\beta\hat{y} + \mu_1 + \frac{\epsilon r}{k}\hat{y} + \tau + \mu_2\right)(\beta\hat{y} + \mu_1 + \mu_3)\left(\frac{\epsilon r}{k}\hat{y} + \tau + \mu_1 + \mu_3\right)
$$

$$
+ \mu_3(\tau + \mu_2)\left(\frac{\epsilon r}{k}\hat{y} + \tau + \mu_1 + \mu_3\right) + \beta\tau\left(\sigma\beta - \frac{\epsilon r}{k}\right)\hat{x}\hat{y}
$$

$$
= -\left(\beta\hat{y} + \mu_1 + \frac{\epsilon r}{k}\hat{y}\right)(\beta\hat{y} + \mu_1 + \mu_3)\left(\frac{\epsilon r}{k}\hat{y} + \tau + \mu_1 + \mu_3\right)
$$

$$
- (\tau + \mu_2)(\beta\hat{y} + \mu_1)\left(\frac{\epsilon r}{k}\hat{y} + \tau + \mu_1 + \mu_3\right) + \beta\tau\left(\sigma\beta - \frac{\epsilon r}{k}\right)\hat{x}\hat{y}
$$

$$
< 0.
$$

Lastly, we consider the determinant of $J(\widehat{P})$. We compute

$$
\det(J(\widehat{P})) = \det\begin{bmatrix} -\beta\hat{y} - \mu_1 & 0 & -\beta\hat{x} \\ (\sigma\beta - \frac{\epsilon r}{k})\hat{y} & -\frac{\epsilon r}{k}\hat{y} - \tau - \mu_2 & \frac{\mu_3}{\tau}(\tau + \mu_2) \\ 0 & \tau & -\mu_3 \end{bmatrix}
$$

$$
= \hat{y}\left[-\frac{\epsilon r\beta\mu_3}{k}\hat{y} - \frac{\epsilon r\mu_1\mu_3}{k} - \beta\tau\left(\sigma\beta - \frac{\epsilon r}{k}\right)\hat{x}\right],
$$

$$
= \frac{\epsilon r\mu_3}{k}\hat{y}\left[-\mu_1 - \frac{k\beta\tau}{\epsilon r\mu_3}\left[2\left(\sigma\beta - \frac{\epsilon r}{k}\right)\hat{x} + \epsilon r - \frac{\mu_3}{\tau}(\tau + \mu_2)\right]\right]
$$

$$
= \frac{\epsilon r\mu_3}{k}\hat{y}\left[f_1'(\hat{x}) - f_2'(\hat{x})\right]
$$

$$
\begin{cases} < 0 & \text{if } f_1'(\hat{x}) - f_2'(\hat{x}) < 0, \text{ i.e. when } \hat{x} = x_1 \text{ or } \bar{x}, \\ > 0 & \text{if } f_1'(\hat{x}) - f_2'(\hat{x}) > 0, \text{ i.e. when } \hat{x} = x_2. \end{cases}
$$

We see that $\det(J(\hat{P}))$ changes sign depending on the sign of $f_1'(\hat{x}) - f_2'(\hat{x})$ and thus may be used to distinguish the stability properties in the case when two distinct chronic-infection equilibria exist. When $R_0 > R_0(\sigma_0)$, the chronic-infection equilibrium P_1 exists in $\overset{\circ}{\Gamma}$ and $\det(J(P_1)) < 0$. Hence, the conditions of Lemma A hold and we may conclude that P_1 is locally asymptotically stable whenever it exists. When $R_0(\sigma_0) < R_0 < 1$, a second chronic-infection equilibrium P_2 is also found in $\overset{\circ}{\Gamma}$ but, as $\det(J(P_2)) > 0$, P_2 is unstable. In this case, it can be shown that $\dim W_{\text{loc}}^s(P_2) = 2$.   □

Proof of Theorem 4.3 Assume that (A_4) holds. Let $p(t) = (x(t), u(t), y(t))$ be a non-constant periodic solution of model (1) with least period $\omega > 0$ and let $\gamma = \{p(t) : 0 \le t < \omega\}$ be its orbit. Consider the 3×3 non-constant invertible matrix

$$
A = A\big(x(t), u(t), y(t)\big) = \begin{bmatrix} 1 & 0 & 0 \\ 0 & \frac{u(t)}{y(t)} & 0 \\ 0 & 0 & \frac{1}{\sigma}\frac{u(t)}{y(t)} \end{bmatrix}.
$$

Compute $B = A_f A^{-1} + A J^{[2]} A^{-1}$, where $A_f = (DA) \cdot f$ or equivalently, A_f denotes the matrix obtained by replacing each entry in A with its directional derivative in the direction of the vector field f for model (1). Write B as a block matrix

$$B = \left[\begin{array}{c|c} B_{11} & B_{12} \\ \hline B_{21} & B_{22} \end{array}\right],$$

where

$$B_{11} = -\beta y - \mu_1 - \frac{\epsilon r}{k} y - \tau - \mu_2,$$

$$B_{12} = \left[\left[\sigma\beta x + \epsilon r\left(1 - \frac{x+u}{k}\right)\right]\frac{y}{u} \quad \sigma\beta\frac{xy}{u}\right], \qquad B_{21} = \left[\begin{array}{c} \tau\frac{u}{y} \\ 0 \end{array}\right],$$

$$B_{22} = \left[\begin{array}{cc} \frac{u'}{u} - \frac{y'}{y} - \beta y - \mu_1 - \mu_3 & 0 \\ \frac{1}{\sigma}(\sigma\beta - \frac{\epsilon r}{k})y & \frac{u'}{u} - \frac{y'}{y} - \frac{\epsilon r}{k}y - \tau - \mu_2 - \mu_3 \end{array}\right].$$

Let $|\cdot|_1$ denote the standard ℓ_1-norm on Euclidean space and select the vector norm $|\cdot|$ on $\mathbb{R}^3 \cong \mathbb{R}^{\binom{3}{2}}$ defined by

$$\left|(v, w)\right| := \max\left\{|v|_1, |w|_1\right\}, \quad \text{for } (v, w) \in \mathbb{R} \times \mathbb{R}^2.$$

The Lozinskiĭ measure $\mu(B)$ (Coppel 1965; Li and Muldowney 1996) associated to $|\cdot|$ may be estimated by

$$\mu(B) \le \sup\{g_1, g_2\},$$

where

$$g_1 = \mu_1(B_{11}) + |B_{12}| = \frac{u'}{u} - \beta y - \mu_1 - \frac{\epsilon r}{k}y \le \frac{u'}{u} - \mu_1,$$

and

$$g_2 = |B_{21}| + \mu_1(B_{22}) = \frac{u'}{u} + \max\left\{-\mu_1 - \frac{1}{\sigma}\left(2\sigma\beta - \frac{\epsilon r}{k}\right)y, -\frac{\epsilon r}{k}y - \tau - \mu_2\right\}$$

$$\le \frac{u'}{u} + \max\{-\mu_1, -\tau - \mu_2\}.$$

Hence,

$$\mu(B) = \mu\left(A_f A^{-1} + A J^{[2]} A^{-1}\right) \le \frac{u'}{u} - \bar{b}, \quad \text{where } \bar{b} = \min\{\mu_1, \tau + \mu_2\} > 0.$$

Next, integrate $\mu(B)$ over one period ω to obtain

$$\int_0^\omega \mu(B)\, ds \le \int_0^\omega \left(\frac{u'(s)}{u(s)} - \bar{b}\right) ds = \log u(s)|_{s=0}^\omega - \bar{b}s|_{s=0}^\omega = -\bar{b}\omega$$

$$< 0 \quad \text{for all } t > 0.$$

Thus, the second compound matrix $J^{[2]}(p(t))$ is asymptotically stable. It follows from Theorem A that the non-constant periodic orbit $p(t)$ is orbitally asymptotically stable with asymptotic phase. Since model (1) is cooperative in Γ by Proposition 4.1, any closed orbits must be non-attracting (Hirsch 1982, Theorem 2.1, or Smith 1995, Theorem 2.2). This contradiction precludes the existence of periodic trajectories in the feasible region Γ. □

Proof of Theorem 4.4 We need to show that the ω-limit set of any trajectory in $\mathring{\Gamma}$ consists of a single equilibrium. Since model (1) is cooperative, there are only two possibilities for the structure of its ω-limit sets. In particular, for a trajectory starting from $y_0 \in \mathring{\Gamma}$, either (i) $\omega(y_0)$ contains an equilibrium, or (ii) $\omega(y_0)$ is a non-attracting periodic orbit. Due to the non-existence of closed orbits in Γ proved in Theorem 4.3, it follows that every compact ω-limit set must contain an equilibrium.

If $P_0 \in \omega(y_0)$, then $\omega(y_0) = \{P_0\}$ since P_0 is locally asymptotically stable. Similarly, $P_1 \in \omega(y_0)$ implies $\omega(y_0) = \{P_1\}$.

Suppose that $P_2 \in \omega(y_0)$ and $\omega(y_0) \neq \{P_2\}$. Then, by Lemma 2.1 of Butler and Waltman (1986), $\omega(y_0)$ contains points on the unstable manifold $W^u(P_2)$ of P_2. Since $W^u(P_2)$ is 1-dimensional, it must be a hetero-clinic orbit connecting P_2 with P_0 or P_1 (Smith 1998, Theorem 2.8). Since $W^u(P_2)$ and $\omega(y_0)$ are invariant and $\omega(y_0)$ is compact, $\overline{W^u(P_2)} \subset \omega(y_0)$, and thus $\omega(y_0)$ contains either P_0 or P_1, contradicting the asymptotic stability of P_0 or P_1. Therefore, $\omega(y_0) = \{P_2\}$. □

References

Asquith, B., Zhang, Y., Mosley, A. J., de Lara, C. M., Wallace, D. L., Worth, A., Kaftantzi, L., Meekings, K., Griffin, G. E., Tanaka, Y., Tough, D. F., Beverly, P. C., Taylor, G. P., Macallan, D., & Bangham, C. R. M. (2007). In vivo T lymphocyte dynamics in humans and the impact of human T-lymphotropic virus 1 infection. *Proc. Natl. Acad. Sci. USA*, *104*, 8035–8040.

Asquith, B., & Bangham, C. R. M. (2007). Quantifying HTLV-I dynamics. *Immunol. Cell Biol.*, *85*, 280–286.

Asquith, B., Mosley, A. J., Barfield, A., Marshall, S. E. F., Heaps, A., Goon, P., Hanon, E., Tanaka, Y., Taylor, G., & Bangham, C. R. M. (2005). A functional CD8$^+$ cell assay reveals individual variation in CD8$^+$ cell antiviral efficacy and explains differences in human T-lymphotropic virus type 1 proviral load. *J. Gen. Virol.*, *86*, 1515–1523.

Asquith, B., & Bangham, C. R. M. (2008). How does HTLV-I persist despite a strong cell-mediated immune response? *Trends Immunol.*, *29*, 4–11.

Bangham, C. R. M. (2000). HTLV-1 infections. *J. Clin. Pathol.*, *53*, 581–586.

Bangham, C. R. M., Meekings, K., Toulza, F., Nejmeddine, M., Majorovits, E., Asquith, B., & Taylor, G. (2009). The immune control of HTLV-I infection: selection forces and dynamics. *Front. Biosci.*, *14*, 2889–2903.

Bangham, C. R. M., & Osame, M. (2005). Cellular immune response to HTLV-1. *Oncogene*, *24*, 6035–6046.

Boxus, M., & Willems, L. (2009). Mechanisms of HTLV-I persistence and transformation. *Br. J. Cancer*, *101*, 1497–1501.

Butler, G., & Waltman, P. (1986). Persistence in dynamical systems. *J. Differ. Equ.*, *63*, 255–263.

Coppel, W. A. (1965). *Stability and asymptotic behaviour of differential equations*. Boston: Heath.

Fiedler, M. (1974). Additive compound matrices and an inequality for eigenvalues of symmetric stochastic matrices. *Czechoslov. Math. J.*, *24*, 392–402.

Gallo, R. C. (2005). The discovery of the first human retrovirus: HTLV-1 and HTLV-2. *Retrovirol*, *2*, 17–23.

Gómez-Acevedo, H., & Li, M. Y. (2005). Backward bifurcation in a model for HTLV-I infection of CD4$^+$ T cells. *Bull. Math. Biol.*, *67*, 101–114.

Hirsch, M. W. (1982). Systems of differential equations which are competitive or cooperative. I: limit sets. *SIAM J. Math. Anal.*, *13*, 167–179.

Kirschner, D., & Webb, G. F. (1996). A model for treatment strategy in the chemotherapy of AIDS. *Bull. Math. Biol.*, *58*, 367–390.

Li, M. Y., & Muldowney, J. S. (1996). A geometric approach to global-stability problems. *SIAM J. Math. Anal.*, *27*, 1070–1083.

Li, M. Y., & Wang, L. (1998). A criterion for stability of matrices. *J. Math. Anal. Appl.*, *225*, 249–264.

Lim, A. G. (2010). Mathematical modelling of HTLV-I infection: a study of viral persistence in vivo. M.Sc. thesis, University of Alberta.

Matsuoka, M., & Green, P. L. (2009). The HBZ gene, a key player in HTLV-I pathogenesis. *Retrovirol*, *6*, 71.

McCluskey, C. C., & van den Driessche, P. (2004). Global analysis of two tuberculosis models. *J. Dyn. Differ. Equ.*, *16*, 139–166.

Meekings, K. N., Leipzig, J., Bushman, F. D., Taylor, G. P., & Bangham, C. R. M. (2008). HTLV-I integration into transcriptionally active genomic regions is associated with proviral expression and with HAM/TSP. *PLoS Pathog.*, *4*, e1000027.

Mortreux, F., Gabet, A. S., & Wattel, E. (2003). Molecular and cellular aspects of HTLV-I associated leukemogenesis in vivo. *Leukemia*, *17*, 26–38.

Mosley, A. J., & Bangham, C. R. M. (2009). A new hypothesis for the pathogenesis of Human T-lymphotropic virus type 1 associated myelopathy/tropical spastic paraparesis. *Biosci. Hypotheses*, *2*, 118–124.

Muldowney, J. S. (1990). Compound matrices and ordinary differential equation. *Rocky Mt. J. Math.*, *20*, 857–872.

Nelson, P. W., Murray, J. D., & Perelson, A. S. (2000). A model of HIV-1 pathogenesis that includes an intracellular delay. *Math. Biosci.*, *163*, 201–215.

Nowak, M. A., & May, R. M. (2000). *Virus dynamics: mathematical principles of immunology and virology*. London: Oxford University Press.

Perelson, A. S. (1989). Modeling the interaction of the immune system with HIV. In C. Castillo-Chavez (Ed.), *Lect. notes biomath: Vol. 83. Mathematical and statistical approaches to AIDS epidemiology* (pp. 350–370). Berlin: Springer.

Perelson, A. S. (2002). Modelling viral and immune system dynamics. *Nat. Rev. Immunol.*, *2*, 28–36.

Proietti, F. A., Carneiro-Proietti, A. B. F., Catalan-Soares, B. C., & Murphy, E. L. (2005). Global epidemiology of HTLV-I infection and associated diseases. *Oncogene*, *24*, 6058–6068.

Saito, M., Matsuzaki, T., Satou, Y., Yasunaga, J., Saito, K., Arimura, K., Matsuoka, M., & Ohara, Y. (2009). In vivo expression of the HBZ gene of HTLV-I correlates with proviral load, inflammatory markers and disease severity in HTLV-I associated myelopathy/tropical spastic paraparesis (HAM/TSP). *Retrovirol*, *6*, 19.

Shiraki, H., Sagara, Y., & Inoue, Y. (2003). Cell-to-cell transmission of HTLV-I. In *Two decades of adult T-cell leukemia and HTLV-I research* (pp. 303–316). Tokyo: Japan Scientific Societies Press.

Smith, H. L. (1998). Systems of ordinary differential equations which generate an order preserving flow. A survey of results. *SIAM Rev.*, *30*, 87–113.

Smith, H. L. (1995). *Mathematical surveys and monographs: Vol. 41. Monotone dynamical systems: an introduction to the theory of competitive and cooperative systems*. Providence: American Mathematical Society.

Wattel, E., Cavrois, M., Gessain, A., & Wain-Hobson, S. (1996). Clonal expansion of infected cells: a way of life for HTLV-I. *J. Acquir. Immune Defic. Syndr.*, *13*, S92–S99.

Wodarz, D., Nowak, M. A., & Bangham, C. R. M. (1999). The dynamics of HTLV-I and the CTL response. *Immunol. Today*, *20*, 220–227.